ISSN: 0003-6935

Applied Optics

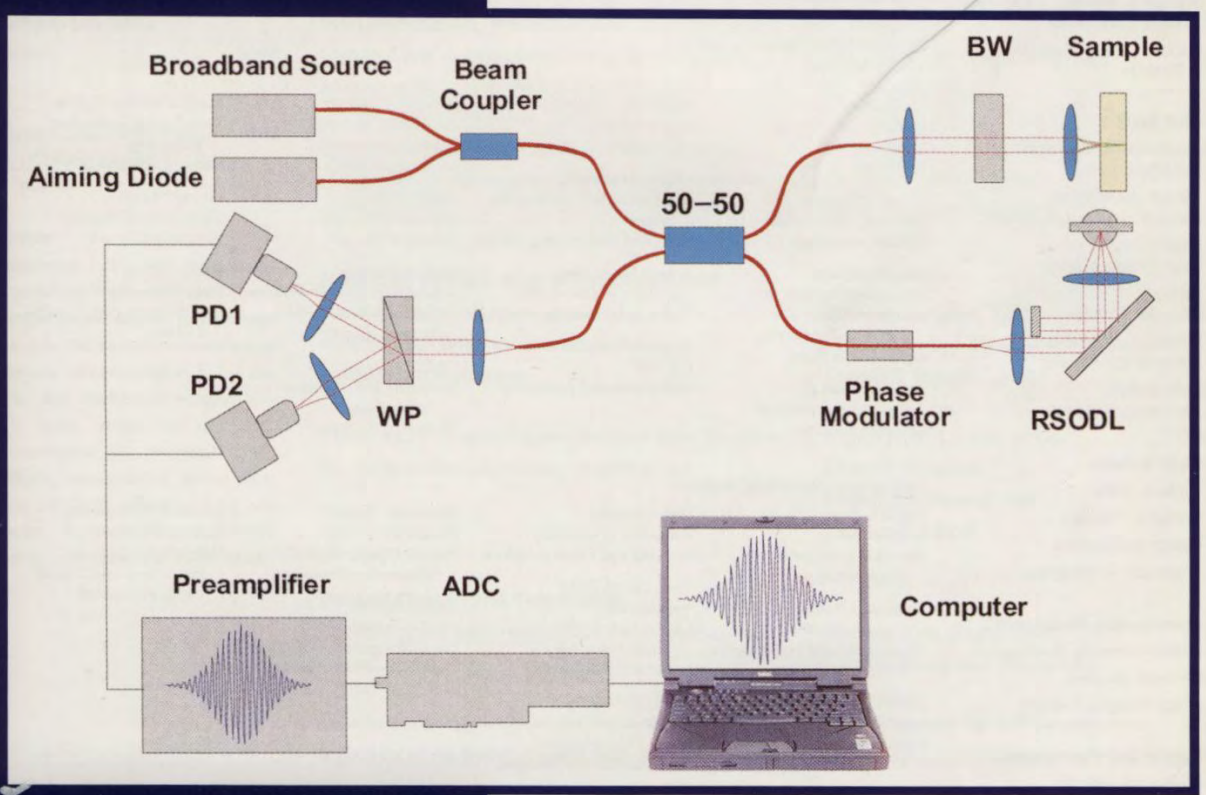

OSA®
Optical Society of America

10 June 2004

Applied Optics

Manuscript Review Office: *Applied Optics*, Manuscript Office, Optical Society of America, 2010 Massachusetts Avenue, NW, Washington, D.C. 20036-1023 (202) 416-1918. Executive Office/Office of the Publisher:Optical Society of America, 2010 Massachusetts Avenue, NW, Washington, D.C. 20036-1023 (202) 223-8130. *Applied Optics* is printed in the USA.

Applied Optics

Volume 43
Number 17
10 June 2004

www.osa.org

Information Pages

Departments

Cover

Schematic of the polarization-maintaining fiber-based dual-channel optical low-coherence reflectometer used for the optical measurement of glucose concentration in turbid media. BW, birefringent wedges; 50–50, beam splitter; PD1 and PD2, photometers; WP, Wollaston prism; RSODL, rapid-scanning optical delay line; and ADC, analog-to-digital converter. For more details, see the paper by Larin *et al.*, pp. 3408–3414.

OPTICAL TECHNOLOGY AND BIOMEDICAL OPTICS

OSA®
Optical Society of America

INFORMATION PROCESSING

LASERS, PHOTONICS, AND ENVIRONMENTAL OPTICS

 Applied Optics (ISSN 0003-6935) is published three times a month by the Optical Society of America, 2010 Massachusetts Avenue, NW, Washington, DC 20036-1023. CODEN: APOPAI. USPS Publication No. 879520. 2004 subscription rates (domestic) per year (paper or microfiche): $134.00 for OSA members; nonmember and library subscriptions: $2680.00. Periodicals postage paid at Washington, DC 20066-9998 and at additional mailing offices. POSTMASTER: Send address changes to *Applied Optics*, 2010 Massachusetts Avenue, NW, Washington, DC 20036-1023. **Subscriptions, missing copies, and change of address:** Optical Society of America, Fulfillment Services, 2010 Massachusetts Avenue, NW, Washington, DC 20036-1023; (202) 416-1907; FAX (202) 416-6130. Back number, single-issue, and foreign rates available on request. *Applied Optics*® is a registered trademark of OSA.

TOPS Trends in Optics & Photonics Series

something for every

biomedical optics

color & vision

information processing

optical science

optical technology

optical networking

photonics

quantum electronics

lasers

Trends in Optics and Photonics Series (TOPS) benefits the individual by providing...

- convenient and affordable up-to-date information for students, researchers, practitioners, and industry professionals.
- comprehensive updates on the latest breakthroughs in technology.

and benefits companies by providing...

- an up-close view of the latest engineering practices and tools that drive products to market faster.
- new research results enabling companies to reduce costs and improve their manufacturing process.

TOPS is a compilation of meeting abstracts and digest papers presented at OSA-sponsored conferences, offering indispensable insights into all fields of optics. TOPS-Proceedings include expanded papers and may include reprints of journal articles and other value-added material.

For a complete listing of volumes and order information visit www.osa/bookstore.
For more information contact Alan N. Tourtlotte, Associate Publisher at atourt@osa.org

OSA
Optical Society of America

a-Si:H/SiO_2 multilayer films fabricated by radio-frequency magnetron sputtering for optical filters

Hidehiko Yoda, Kazuo Shiraishi, Yuji Hiratani, and Osamu Hanaizumi

We examined the optical properties of *a*-Si:H/SiO_2 multilayer films fabricated by radio-frequency magnetron sputtering for optical bandpass filters (BPFs). Because of the high refractive-index contrast between *a*-Si:H and SiO_2, the total number of layers of an *a*-Si:H/SiO_2 multilayer can be relatively small. We obtained an *a*-Si:H refractive index of 3.6 at $\lambda = 1550$ nm and its extinction coefficient $k < 1 \times 10^{-4}$ and confirmed by Fourier-transform infrared spectroscopy that such small k is influenced by the Si–H bonding in the film. We fabricated *a*-Si:H/SiO_2 BPFs by using *in situ* optical monitoring. Thermal tuning of *a*-Si:H/SiO_2 BPF upon a silica substrate was also performed, and a thermal tunability coefficient of 0.07 nm/°C was obtained.

OCIS codes: 310.6860, 310.1860, 310.3840, 230.4170, 060.4230.

1. Introduction

Dense–coarse wavelength-division multiplexing (WDM) is widely used in optical fiber communication today. Key components of the system are narrow–wide optical bandpass filters (BPFs) with flat-topped spectra, which are used to extract a specific signal from among a number of WDM signals. The BPFs are formed from alternating multilayer films of two dielectric materials such as Ta_2O_5/SiO_2 and TiO_2/SiO_2 with high–low refractive indices. However, a Ta_2O_5/SiO_2 BPF requires a multilayer with 50 to hundreds of layers,[1,2] which makes fabricating this material difficult because a stack of films causes thickness errors or film stress.[2] The total number of layers of a multilayer can be reduced by choice of a pair of materials with high refractive-index contrast, which is defined as the high index of one material divided by the low index of another. Two such pairs of materials are hydrogenated amorphous silicon (*a*-Si:H) and silicon dioxide (SiO_2), and *a*-Si:H and silicon nitride (Si_3N_4),[3] of which the refractive-index contrasts are 2.5 and 2.0, respectively, whereas the index contrast of Ta_2O_5/SiO_2 is 1.45. Therefore *a*-Si:H/SiO_2 multilayer films have the major advantage that the total number of layers of the multilayer is almost half of that of Ta_2O_5/SiO_2 multilayer films. We studied Si/SiO_2 multilayer films for optical devices such as laminated polarized splitters and filters by using radio-frequency (RF) magnetron sputtering equipment with a Si target.[4,5] In equipment that employs a Si target, hydrogenated amorphous silicon oxide (*a*-SiO_x:H, $0 \le x \le 2$) with refractive indices of 1.44 (SiO_2) to 3.6 (*a*-Si:H) is deposited by control of O_2 gas flow. Refractive-index-controllable materials such as *a*-SiO_x:H and *a*-SiN_x:H can be applied to fabrication of rugate filters.[6,7]

In this study we examined the optical properties of *a*-Si:H and SiO_2 films fabricated by RF magnetron sputtering and determined deposition conditions for *a*-SiO_x:H films as well. We fabricated an *a*-Si:H/SiO_2 BPF with 27 layers and demonstrated its thermal tuning. We also found that the *a*-SiO_x:H film shows promise for fabricating rugate filters by control of oxidation parameter x.

2. Optical Properties of *a*-Si:H and SiO_2 Films

It is necessary to know the optical properties and microstructure of filter materials *a*-Si:H and SiO_2 to predict filter performance, so we deposited *a*-Si:H and SiO_2 films by using RF magnetron sputtering equipment, as shown in Fig. 1. The sputtering equipment consists of a RF generator operating at a frequency of 13.56 MHz; a silicon Si target on a magnet; two mass-flow controllers for argon, including hydrogen (Ar + H_2) and oxygen (O_2) gases; a heater; and a thermo-

H. Yoda and K. Shiraishi are with the Graduate School of Engineering, Utsunomiya University, 7-1-2 Yoto, Utsunomiya 321-8585, Japan. Y. Hiratani and O. Hanaizumi are with the Faculty of Engineering, Gunma University, 1-5-1 Tenjin-Cho, Kiryu 376-8515, Japan. H. Yoda's e-mail address is yoda@cc.utsunomiya-u.ac.jp.

Received 8 September 2003; revised manuscript received 3 March 2004; accepted 22 March 2004.

0003-6935/04/173548-07$15.00/0

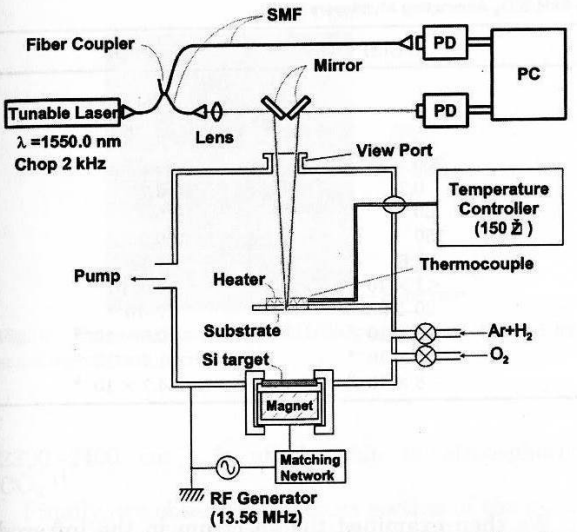

Fig. 1. RF magnetron sputtering equipment and optical monitoring system: PDs, photodetectors; PC, personal computer; SMF, single-mode fiber.

couple for substrate-temperature control. When $Ar + H_2$ gas flows at an appropriate gas pressure and RF power, Ar and H ions are formed, and then the Si target is sputtered. The sputtered Si particles fly and react with H ions, and as a result a-Si:H film is deposited onto the substrate, which is placed 10 cm above the Si target. In our experiment the a-Si:H film had sufficiently low absorption in the near-infrared region to form optical filters. If 100% Ar gas were used instead of the $Ar + H_2$ gas mixture, a-Si film with high absorption in the region would be deposited. Next, when O_2 gas flows with $Ar + H_2$ gas, sputtered Si particles react with O ions and then SiO_2 film is deposited onto the substrate.

First we examined two parameters, a-Si:H refractive index at wavelength $\lambda = 1550$ nm and O_2 gas flow for the SiO_2 film, under various conditions of RF power, gas pressure, and O_2 gas flow ratio. Amorphous Si:H film was deposited onto silica substrates to a thickness of several micrometers. The refractive index can be estimated from the peak wavelengths in transmittance (or reflectance) and the film thickness under a reasonable assumption of an extinction coefficient equal to 0. Figure 2 shows the refractive index of a-Si:H and its oxide (a-SiO_x:H, $0 < x \leq 2$) films at $\lambda = 1550$ nm as functions of RF power (300 or 500 W) and gas flow ratio $O_2/(Ar + H_2 + O_2)$. Here, total gas ($Ar + H_2 + O_2$) flow, gas pressure, and substrate temperature were kept at 20 SCCM, 1.0 Pa, and 150 °C, respectively, where SCCM denotes cubic centimeters per minute at STP. The refractive index of a-Si:H was obtained at an O_2 gas flow ratio of 0 in Fig. 2, which is read as being ~3.6. As the O_2 gas flow ratio increases, the refractive index of a-SiO_x:H film gradually decreases and suddenly falls off to the SiO_2 refractive index (1.44) at a critical value. We know that this critical value varies with

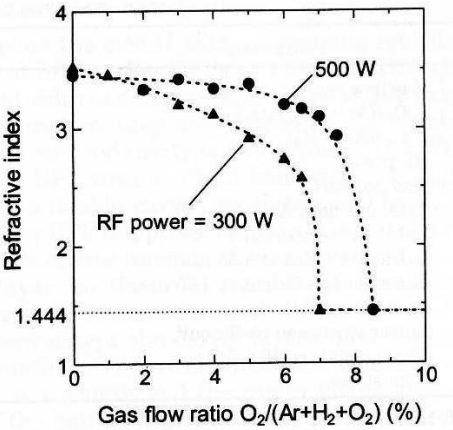

Fig. 2. Refractive index of a-Si:H and its oxide films at $\lambda = 1550$ nm as functions of RF power and O_2 gas flow ratio $O_2/(Ar + H_2 + O_2)$ at a gas pressure of 1.0 Pa.

each RF power. Figure 3 shows the refractive indices of a-Si:H and a-SiO_x:H films at $\lambda = 1550$ nm as functions of gas pressure (0.7 or 1.0 Pa) and O_2 gas flow ratio. Here the total gas flow, RF power, and substrate temperature are 20 SCCM, 300 W, and 150 °C, respectively. For a gas pressure of 0.7 Pa the refractive index decreases gradually from 3.6 to 2.2 as the O_2 gas flow ratio is increased from 0% to 9%. The gradual and wide change in the refractive index is useful for controlling the refractive index of a-SiO_x:H and for rugate filter applications, so we decided to use the deposition conditions listed in Table 1, setting the O_2 gas flow ratio for SiO_2 at 20% to have enough margin for error.

Next we deposited a-Si:H film under the conditions in Table 1 and examined its refractive index and the dependence of its extinction coefficient on wavelength. We measured the film spectrum, both transmittance and reflectance, by using a spectrophotometer with a halogen lamp as the light source and with an output

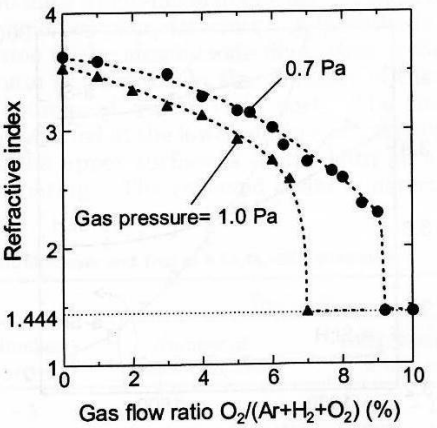

Fig. 3. Refractive index of a-Si:H and its oxide films at $\lambda = 1550$ nm as functions of gas pressure and O_2 gas flow ratio $O_2/(Ar + H_2 + O_2)$ at a RF power of 300 W.

Table 1. Deposition Conditions for a-Si:H/SiO_2 Alternating Multilayers

Parameter	Unit	a-Si:H	SiO_2
Gas flow ratio			
$O_2/(Ar + H_2 + O_2)$	%	0	20
$H_2/(Ar + H_2)$	%	5	5
RF power	W	300	300
Gas pressure	Pa	0.7	0.7
Total gas flow, $Ar + H_2 + O_2$	SCCM	20	20
Substrate temperature	°C	150	150
Refractive index at 1.55 μm		3.6	1.44
Extinction coefficient at 1.55 μm		$<1 \times 10^{-4}$	$<1 \times 10^{-5}$
Deposition rate	nm/min	20–24	7–10
Linear expansion coefficient[a]	$°C^{-1}$	1×10^{-6}	0.5×10^{-6}
Thermo-optic coefficient[b]	$°C^{-1}$	3×10^{-4}	1.2×10^{-5}
Film stress	dyn/cm^2	-8×10^{-9}	-4.7×10^{-9}

[a]Ref. 15.
[b]Ref. 16.

power stability of ±0.5%. The a-Si:H film thickness was 2880 ± 15 nm, which was measured by a surface profilometer. The a-Si:H refractive index and extinction coefficient with error bars could then be calculated from the data of film spectrum and thickness.

Figure 4 shows the a-Si:H refractive index (n) and extinction coefficient (k) with error bars as a function of wavelength. From Fig. 4 the a-Si:H refractive index at $\lambda = 1550$ nm is estimated to be $n = 3.59 \pm 0.015$. The a-Si:H extinction coefficient at $\lambda = 1550$ nm is estimated to be approximately $k < 1 \times 10^{-4}$. The coefficient of the a-Si:H film is smaller by 1 order of magnitude than that in the nonhydrogenated a-Si film with $k = 5 \times 10^{-3}$. The value of $k < 1 \times 10^{-4}$ is sufficiently small to permit fabrication of multiple-cavity BPFs (which correspond to a loss of <0.5 dB). Note that SiO_2 films were deposited upon the silica substrate with $n = 1.44$ and $k < 10^{-5}$ at $\lambda = 1550$ nm but that there was almost no change in the SiO_2 film spectrum compared with the silica substrate spectrum, so we regarded the optical constant of the SiO_2 film as being the same as that of the silica substrate.

We then examined the spectrum in the infrared region to confirm the existence of hydrogen in the film. Amorphous Si:H, a-Si, and SiO_2 films were deposited onto a silicon substrate that had low absorption in the infrared region. The spectrum was measured by Fourier-transform infrared spectroscopy (FTIR) to ensure that the film was sufficiently thin for the FTIR spectrum not to suffer interference in the infrared region. The FTIR spectrum is shown in Fig. 5. The a-Si:H spectrum had Si–H absorption peaks centered at 630 and 2000 cm^{-1}.[8] The absorption peaks of Si–H are not shown in the a-Si and SiO_2 spectra. This result means that the a-Si:H film is certainly hydrogenated and that the SiO_2 film is not hydrogenated. Therefore, Si–H bonding in the film is the reason for the 1-order-of-magnitude greater loss of a-Si:H film than of a-Si film. The absorption peaks near 450, 800, and 1060 cm^{-1} are associated with the Si–O stretching band.[9] The noise near 1350–1900 cm^{-1} is due to the presence of atmospheric water in the FTIR system.[10] The peak near

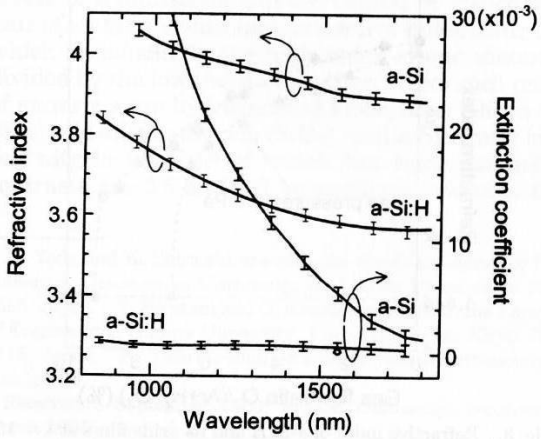

Fig. 4. Refractive index and extinction coefficient of a-Si:H and Si:H as functions of wavelength.

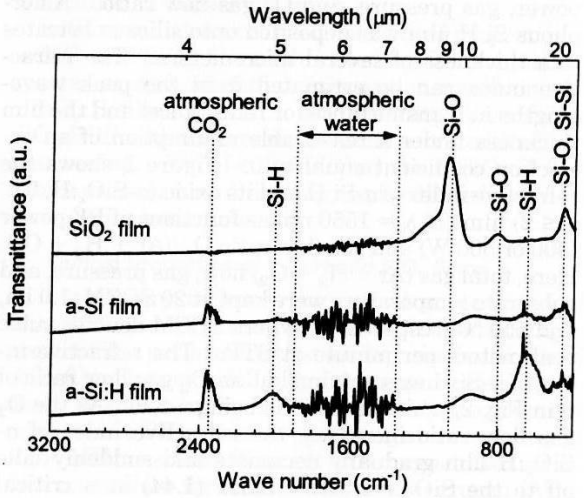

Fig. 5. FTIR spectrum.

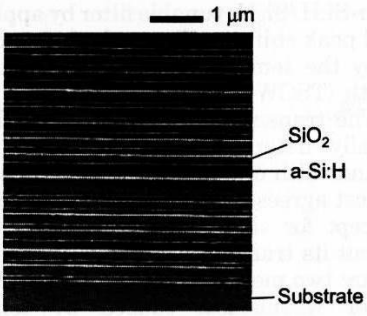

Fig. 6. Cross section of an a-Si:H/SiO_2 multilayer obtained by scanning-electron microscopy.

2300–2400 cm^{-1} is attributable to atmospheric CO_2.[11]

Finally, we observed the cross section of the a-Si:H/SiO_2 alternating multilayer by scanning-electron microscopy to confirm the homogeneity and high density of the deposited films. We fabricated the a-Si:H/SiO_2 alternating multilayer by switching the O_2 gas flow on and off at a constant interval, using the sputtering equipment shown in Fig. 1. Before observation, we wet etched the a-Si:H layers by using a 34% KOH solution to distinguish between a-Si:H and SiO_2 layers. A scanning-electron microphotograph of the cross section is shown in Fig. 6, indicating that each film is homogeneous and has a high density of almost 1.

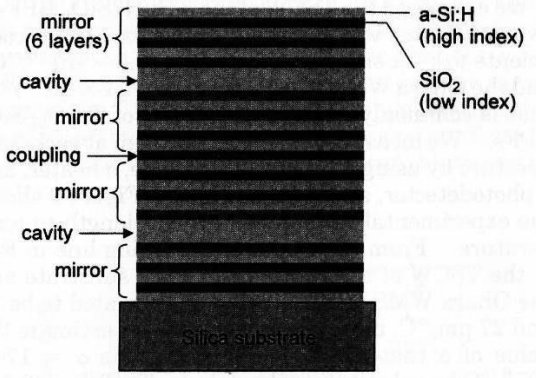

Fig. 7. Structure of an a-Si:H/SiO_2 double-cavity BPF with 27 layers.

3. Application for Optical Filters

We applied the a-Si:H/SiO_2 alternating multilayers to optical BPFs. For BPFs in a dense WDM system the bandwidth and the spectral shape of BPFs are the key parameters; they are decided by the number of mirror layers and cavity layers of the BPF. We fabricated a BPF with a −3-dB bandwidth (Δ_{-3dB}) of 2 nm and a double cavity, as shown in Fig. 7. The multilayer BPF comprises two cavity layers, four mirrors (each mirror consists of six layers) and one coupling layer, so the total number of layers in the multilayer is 27 and the total thickness is ~5 μm. All layers except the cavity layers have a quarter-wavelength ($\lambda/4$) optical thickness, where λ is the design wavelength and the cavity layers are multiples of the half-wavelength ($\lambda/2$) optical thickness.

The total number of layers of the multilayer depends on the multilayer materials used. Table 2 lists the total number of layers calculated for a multilayer structure made from materials such as a-Si:H/SiO_2 and Ta_2O_5/SiO_2. Here the refractive indices of a-Si:H, Ta_2O_5, and SiO_2 are assumed to be 3.6 ($=n_H$), 2.1 ($=n_H$), and 1.44 ($=n_L$) at λ = 1550 nm, respectively. Hence the refractive-index contrast (n_H/n_L) of a-Si:H/SiO_2 and Ta_2O_5/SiO_2 becomes 2.5 and 1.45, respectively. The number of mirror layers and the total number of layers of the multilayer depend on the refractive-index constant. The higher the refractive-index contrast, the smaller the total number of layers. For example, as shown by Table 2, the a-Si:H/SiO_2 multilayer with 2-nm bandwidth and the double cavity (N = 2) needs 27 ($=14 \times 2 - 1$) layers, whereas the Ta_2O_5/SiO_2 multilayer with the same performance needs 59 ($=30 \times 2 - 1$) layers. The smaller total number for the a-Si:H/SiO_2 multilayer is an advantage in fabricating BPFs.

When one is fabricating multilayer BPFs it is important to control the optical thickness of each layer accurately in multiples of $\lambda/4$, so we used an *in situ* optical monitoring system with sputtering equipment, as shown in Fig. 1. This system is composed of a tunable laser diode (spectrum width, 200 MHz at λ = 1550 nm), single-mode fibers, a 1 × 2 optical fiber coupler, and two photodetectors. A laser diode beam propagates in the single-mode fibers and is then incident onto a substrate in the chamber of the sputtering equipment via a view port. The incident beam is reflected at the lower surface of the substrate because the upper surface is coated with an antireflection coating. The reflected beam is detected by

Table 2. Comparison between the Total Number of Layers of an a-Si:H/SiO_2 Multilayer and That of a Ta_2O_5–SiO_2 Multilayer[a]

Channel Spacing (GHz) [nm]	−3 dB Bandwidth (nm)	a-Si:H/SiO_2		Ta_2O_5/SiO_2	
		Number of Mirror Layers	Total Number of Layers	Number of Mirror Layers	Total Number of Layers
1000 [8.0]	5	5	$12N - 1$	11	$24N - 1$
400 [3.2]	2	6	$14N - 1$	14	$30N - 1$
200 [1.6]	1	7	$16N - 1$	16	$34N - 1$

[a] N is the numbers of cavity layers.

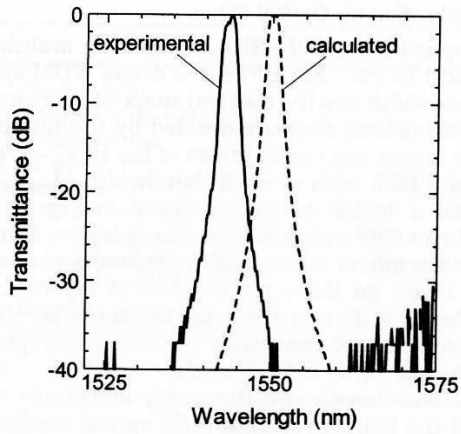

Fig. 8. Experimental and calculated spectra of an a-Si:H/SiO_2 BPF with 27 layers upon a silica substrate.

the photodetector. The intensity of the reflected beam is monitored during a-Si:H/SiO_2 multilayer deposition, so we call it a monitoring beam. The monitoring beam's intensity changes as a sinusoidal function of deposition time, and the change has local extreme peaks at certain times. Just at the deposition time of the local extrema, the film thickness becomes an exact multiple of the $\lambda/4$ optical thickness,[12] so we should switch the gas flow ratio $O_2/(Ar + H_2 + O_2)$ at precisely this moment.

The substrate temperature must be controlled if one is to find the local extreme peak in the optical monitoring change in beam intensity. Substrate temperature must be controlled to stabilize the optical monitoring measurements and to prevent a difference between measurement and theory. Therefore we maintain the substrate temperature constant at 150 °C by using a heater and a thermocouple, as shown in Fig. 1.

For practical use, the spectrum of a BPF must be stable against changes in temperature. However, the thermo-optic coefficient of a-Si:H film is so high that a spectrum shift may occur. Figure 8 shows experimental and calculated transmission spectra of the a-Si:H/SiO_2 BPF fabricated by use of the optical monitoring system. The experimental spectrum was measured at room temperature, so the center wavelength at the transmittance peak is shifted shorter than $\lambda = 1550$ nm. Damash *et al.* first proposed an a-Si:H/Si_3N_4 tunable filter by applying such a thermal peak shift.[13] The peak shift is clearly explained by the temperature stability of the center wavelength (TSCW) of the BPF, which is described below. The transmission loss at the peak was experimentally determined to be ~0.13 dB. The −3-dB bandwidth of 2 nm in the experimental spectrum almost agrees with that in the calculated spectrum, except for slight distortion of the spectrum shape about its transmission peak.

There are two methods of dealing with the shift of the center wavelength caused by temperature change: One is to reduce the shift for thermal stability and the other is to utilize the shift for applications such as thermally tunable filters. In reducing the shift we should use a proper substrate that has a higher linear expansion coefficient.[14] In Ref. 14 the relationship between the TSCW of a BPF and a substrate expansion coefficient is given by strict equations, but the relationship is not immediately clear from these equations. We therefore derive a simple equation under some approximations (see Appendix A) as follows:

$$\mathrm{TSCW} = \lambda(\delta + C_2\beta - C_1\alpha), \tag{1}$$

where λ is wavelength, δ is the thermo-optic coefficient of the multilayer, α and β are the linear expansion coefficients of the substrate and the multilayer, respectively, and C_1 and C_2 are constants that are not related to the substrate, as shown in Table 3. Equation (1) indicates that the TSCW decreases in proportion to α. Therefore α should be chosen to cancel δ and β such that the TSCW will become zero.

We examined the TSCW of the a-Si:H/SiO_2 BPF on two substrates with different linear expansion coefficients (α): a silica substrate ($\alpha = 0.5 \times 10^{-6}$/°C), and the Ohara WMS-02 substrate ($\alpha = 11 \times 10^{-6}$/°C) that is commonly used in fabrication of Ta_2O_5/SiO_2 BPFs. We measured the BPF spectrum at each temperature by using a tunable laser diode, a heater, and a photodetector, as shown in Fig. 1. Figure 9 shows the experimental ratio of center wavelength to temperature. From the slopes of the fitting line in Fig. 9, the TSCW of the BPF on the silica substrate and the Ohara WMS-02 substrate are estimated to be 72 and 27 pm/°C, respectively. Hence we estimate the value of α that yields TSCW = 0 to be $\alpha = 17 \times 10^{-6}$/°C by substituting the data (α, TSCW) = ($0.5 \times$

Table 3. Material Parameters of a Multilayer and a Substrate

Parameter	Subject	Symbol	Unit	Typical Value
Temperature stability of the center wavelength	BPF upon a substrate	TSCW	pm/°C	0–70
Wavelength	Laser diode	λ	nm	1550
Linear expansion coefficient	Substrate	α	$°C^{-1}$	10^{-6}–10^{-5}
Linear expansion coefficient	Multilayer BPF	β	$°C^{-1}$	10^{-6}
Thermo-optic coefficient normalized by N_0	Multilayer BPF	δ	$°C^{-1}$	10^{-5}
Effective refractive index	Multilayer BPF	N_0		1–3
Poisson ratio	BPF upon a substrate	s		0.1–0.3
Constant	Multilayer BPF	C_1, C_2		0.2–2.6

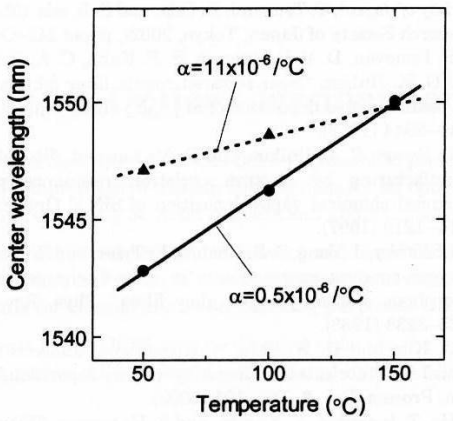

Fig. 9. Temperature stability of the center wavelength of a-Si:H/SiO_2 BPFs upon two substrates with different linear expansion coefficients (α): silica substrate ($\alpha = 0.5 \times 10^{-6}$/°C) and an Ohara WMS-02 substrate ($\alpha = 11 \times 10^{-6}$/°C).

10^{-6}/°C, 72 nm) and (11×10^{-6}/°C, 27 nm) into Eq. (1).

When we use the center wavelength shift for thermal tuning, however, we may use a substrate with α either much smaller than 17×10^{-6}/°C or negative. Figure 10 shows the a-Si:H/SiO_2 BPF spectra for a silica substrate as a function of temperature. The thermal tunability coefficient obtained is ~0.07 nm/°C. For the coefficient of 0.08–0.15 nm/°C reported in Ref. 13 when a-Si:H/Si_3N_4 was used, the measured value 0.07 nm/°C is almost the same. It is noteworthy that the refractive-index contrast of the a-Si:H/SiO_2 multilayer reported here is much higher than that of a-Si:H/Si_3N_4 film. On changing the temperature from 25 to 200 °C, we estimate that the a-Si:H/SiO_2 filter will be able to cover the quarter range 10 nm of the C band. Equation (1) suggests that the use of substrates with negative expansion coefficients ($\alpha < 0$) could increase the thermal tunability coefficient.

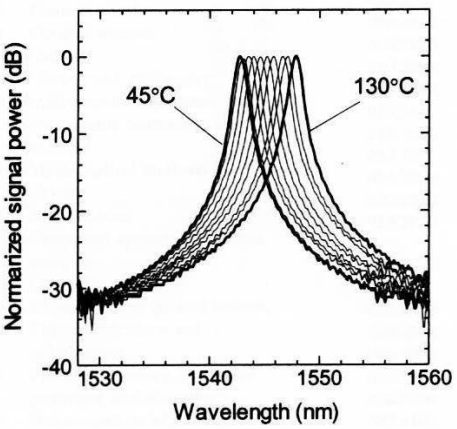

Fig. 10. Transmission spectra of a one-cavity a-Si:H/SiO_2 BPF upon a silica substrate as a function of temperature.

4. Conclusions

We examined the optical properties of a-Si:H/SiO_2 multilayer films fabricated with RF magnetron sputtering for optical BPFs. For RF power 300 W, gas pressure 0.7 Pa, and substrate temperature 150 °C the refractive indices of the a-Si:H and SiO_2 films were 3.6 and 1.44, respectively, at $\lambda = 1550$ nm. Because of high refractive-index contrast between a-Si:H and SiO_2 ($n_H/n_L = 2.5$) compared with that of conventional materials such as Ta_2O_5/SiO_2 ($n_H/n_L = 1.45$), the total number of a-Si:H/SiO_2 multilayer BPFs can be almost half that of a Ta_2O_5/SiO_2 BPF. We also obtained the a-Si:H extinction coefficient $k < 1 \times 10^{-4}$ at $\lambda = 1550$ nm and confirmed by FTIR that such small k is influenced by the Si–H bonding in the film.

We fabricated an a-Si:H/SiO_2 BPF with 27 layers and 2-nm bandwidth by using *in situ* optical monitoring. We investigated the TSCW of this BPF and found that a substrate expansion coefficient of 17×10^{-6}/°C is required for a value of TSCW = 0 to be achieved. The thermal tunability coefficient of the a-Si:H/SiO_2 BPF on a silica substrate was found to be 0.07 nm/°C.

Appendix A

The TSCW of a narrow BPF is given by Eq. (19) of Ref. 14 as follows:

$$\mathrm{TSCW} = \lambda\left(\frac{n_T d_T}{n_0 d_0} - 1\right), \tag{A1}$$

where λ is the center wavelength, n_0 and n_T are the effective refractive indices of the BPF and d_0 and d_T are the physical thicknesses of BPF at temperatures of T_0 and $T_0 + 1$, respectively. n_T and d_T are functions of several parameters, i.e., α, β, δ, and s, which are defined in Table 3. Here we make the following reasonable assumptions when BPF films are deposited by sputtering, ion beam deposition, etc.:

(i) Average packing density of a narrow BPF, $P_0 \cong 1$.

(ii) The values of α, β, δ, $A = 2(1 - 2s)/(1 - s)(\alpha - \beta)$ and $B = 2s/(1 - s)(\alpha - \beta)$ range in order from 10^{-6} to 10^{-4}.

Under assumption (i), Eq. (1) of Ref. 14 becomes $n_0 \cong N_0$. Under assumption (ii), the value of x ($=\alpha$, β, δ, A, B) is much larger than that of x^2, so x^2 can be abbreviated. Under these assumptions, n_T and d_T are simply given by Eqs. (18) and (15) of Ref. 14:

$$n_T \cong \frac{N_0(1 + \delta)(1 + 3\beta) + A}{1 + 3\beta + A} \cong N_0\left(1 + \delta - \frac{N_0 - 1}{N_0} A\right), \tag{A2}$$

$$d_T = d_0(1 - B + \beta). \tag{A3}$$

From Eqs. (A2) and (A3), the TSCW in Eq. (A1) can be rewritten as

$$\mathrm{TSCW} \cong \lambda\left(\delta + \beta - \frac{N_0 - 1}{N_0} A - B\right)$$
$$\cong \lambda(\delta + C_2\beta - C_1\alpha), \tag{A4}$$

$$C_1 = 2 - \frac{2}{N_0}\frac{1 - 2s}{1 - s},$$
$$C_2 = C_1 + 1, \tag{A5}$$

where s and N_0 are Poisson's ratio and the effective refractive index of the BPF, respectively.

The authors thank T. Yasuda and M. Waki, Utsunomiya University, for contributions to the fabrication of multiple-cavity BPFs.

References

1. H. Hagedorn, A. Lots, P. Pecher, and O. Treichel, "Ultra narrow bandpass filters produced by plasma ion assisted deposition," in *Proceedings of Optical Interference Coatings 2001* (Optical Society of America, Washington, D.C., 2001), pp. WA4-1–WA4-3.
2. G. J. Ockenfuss and N. A. O'Brien, "Ultra-low stress coating process: an enabling technology for extreme performance thin film interference filters," in *Optical Fiber Communication Conference* (*OFC*), Vol. 70 of OSA Trends in Optics and Photonics Series (Optical Society of America, Washington, D.C., 2002), pp. FA8-1–FA8-3.
3. R-Y. Tsai, L-C. Kuo, and F. C. Ho, "Amorphous silicon and amorphous silicon nitride films prepared by a plasma-enhanced chemical vapor deposition process as optical coating materials," Appl. Opt. **32,** 5561–5566 (1993).
4. K. Muro and K. Shiraishi, "Poly-Si/SiO_2 laminated walk-off polarizer having a beam-splitting angle of more than 20°," J. Lightwave Technol. **16,** 127–133 (1998).
5. H. Yoda and K. Shiraishi, "Optical wavelength filter using hydrogenated silicon oxide for optical communication," in *Proceedings of the 14th Symposium of the Materials Research Society of Japan*, T. Tsurumi, K. Oda, and S. Ii, eds. (Materials Research Society of Japan, Tokyo, 2002), paper M2–O04-G.
6. E. P. Donovan, D. V. Vechten, A. S. F. Kahn, C. A. Carosella, and G. K. Hubler, "Near infrared rugate filter fabrication by ion beam assisted deposition of $Si_{(1-x)}N_x$ films," Appl. Opt. **28,** 2940–2944 (1989).
7. P. L. Swart, P. V. Bulkin, and B. M. Lacquet, "Rugate filter manufacturing by electron cyclotron resonance plasma-enhanced chemical vapor deposition of SiN_x," Opt. Eng. **36,** 1214–1219 (1997).
8. G. Lucovsky, J. Yang, S. S. Chao, J. E. Tyler, and W. Czubatyj, "Oxygen-bonding environments in glow-discharge-deposited amorphous silicon-hydrogen alloy films," Phys. Rev. B **28,** 3225–3233 (1983).
9. Y. J. Kim and D. W. Shin, "Compositional analysis of SiO_2 optical film fabricated by flame hydrolysis deposition," J. Ceram. Process. Res. **3,** 186–191 (2002).
10. L. He, T. Inokuma, Y. Kurata, and S. Hasegawa, "Vibrational properties of SiO and SiH in amorphous SiO_x:H films ($0 < x < 2.0$) prepared by plasma-enhanced chemical vapor deposition," J. Non-Cryst. Solids **185,** 249–261 (1995).
11. G. Jennings, L. Bluck, A. Wright, and M. Elia, "The use of infrared spectrophotometry for measuring body water spaces," Clin. Chem. (N.Y.) **45,** 1077–1081 (1999).
12. P. Bousquet, A. Fornier, R. Kowalczyk, E. Pelletier, and P. Roche, "Optical filters: monitoring process allowing the autocorrection of thickness errors," Thin Solid Films **13,** 285–290 (1972).
13. L. Domash, E. Ma, N. Nemchuk, and A. Payne, "Tunable thin film filters," in *Optical Fiber Communication Conference* (*OFC*), Vol. 86 of OSA Trends in Optics and Photonics Series (Optical Society of America, Washington, D.C., 2003), pp. 522–524, paper ThM3.
14. H. Takahashi, "Temperature stability of thin-film narrow-bandpass filters produced by ion-assisted deposition," Appl. Opt. **34,** 667–675 (1995).
15. K. Takimoto, A. Fukuta, Y. Yanamoto, N. Yoshida, T. Itoh, and S. Nonomura, "Linear thermal expansion coefficients of amorphous and microcrystalline silicon films," J. Non-Cryst. Solids **299-302,** 314–317 (2002).
16. G. Cocorullo, F. G. Della Corte, L. Moretti, I. Rendina, and A. Rubino, "Measurement of the thermo-optic coefficient of *a*-Si:H at the wavelength of 1500 nm from room temperature to 200 °C," J. Non-Cryst. Solids **299-302,** 310–313 (2002).